Journal of Sound and Vibration 329 (2010) 2384–2394

Contents lists available at ScienceDirect

Journal of Sound and Vibration

journal homepage: www.elsevier.com/locate/jsvi

Beamforming array techniques for acoustic emission monitoring of large concrete structures

Gregory C. McLaskey [a], Steven D. Glaser [a,*], Christian U. Grosse [b]

[a] Department of Civil and Environmental Engineering, University of California, 455 Davis Hall, Berkeley, CA 94720-1710, USA
[b] MPA Department of Non-Destructive Testing and Monitoring Techniques, Universität Stuttgart, 70550 Stuttgart, Germany

ARTICLE INFO

Article history:
Accepted 30 August 2009
The peer review of this article was organised by the Guest Editor
Available online 23 September 2009

ABSTRACT

This paper introduces a novel method of acoustic emission (AE) analysis which is particularly suited for field applications on large plate-like reinforced concrete structures, such as walls and bridge decks. Similar to phased-array signal processing techniques developed for other non-destructive evaluation methods, this technique adapts beamforming tools developed for passive sonar and seismological applications for use in AE source localization and signal discrimination analyses. Instead of relying on the relatively weak P-wave, this method uses the energy-rich Rayleigh wave and requires only a small array of 4–8 sensors. Tests on an in-service reinforced concrete structure demonstrate that the azimuth of an artificial AE source can be determined via this method for sources located up to 3.8 m from the sensor array, even when the P-wave is undetectable. The beamforming array geometry also allows additional signal processing tools to be implemented, such as the VESPA process (VElocity SPectral Analysis), whereby the arrivals of different wave phases are identified by their apparent velocity of propagation. Beamforming AE can reduce sampling rate and time synchronization requirements between spatially distant sensors which in turn facilitates the use of wireless sensor networks for this application.

1. Introduction

When structural damage occurs, a spontaneous release of strain energy creates transient stress waves, known as acoustic emission (AE), which propagate through the material. Acoustic emission has been used for years as a method for passive structural health monitoring [1–5]. The main difference between AE and other methods, such as modal analysis, is that it does not rely on subtle changes in the wave propagation characteristics of the material to detect cracks and flaws. Instead, recorded signals are a direct function of the energy released from local damage mechanisms such as cracking. The signals collected by an acoustic emission sensor depend on both the nature of the mechanism (i.e. what type of crack growth), the nature of the material through which the stress waves propagate, and the characteristics of the sensor and data acquisition system [6]. The goal of quantitative AE analyses is not just to count acoustic emission 'events' but to discriminate between different types or different sources of acoustic emissions and noise, either by their spatial coordinates, their frequency content, amplitude, or by some other means. The beamforming array techniques described in this paper offer a promising and economically feasible method for solving for a key source parameter (direction of arrival)

* Corresponding author. Tel.: +1 510 642 1264.
E-mail address: glaser@berkeley.edu (S.D. Glaser).

0022-460X/$ - see front matter © 2009 Elsevier Ltd. All rights reserved.
doi:10.1016/j.jsv.2009.08.037

on large, plate-like concrete structures such as bridge decks. When two or more beamforming arrays are combined, the source can be located in two dimensions [7].

In theory, it is possible to gain useful, quantitative information such as precise AE source locations and source kinematics from waveform analysis. Although quantitative methods have been successfully applied in the laboratory [8–11], it is impossible for the AE method to achieve the same functional level on large concrete structures without the use of a dense array of sensors and expensive data acquisition systems which could begin to rival the cost of the structure itself. The beamforming source location and signal discrimination techniques described in this paper are analysis tools and testing techniques which are intended to strike a balance between feasibility and utility; they can be more economically feasible and are better suited to the scale and the needs of large structures in civil engineering field applications than traditional methods.

Source location of structural damage is one of the most important pieces of information to be gained from the AE method. The rough localization of damage on a large structure can direct further, more detailed, non-destructive analyses to the proper location. Conventional AE monitoring techniques use sparse, distributed arrays and require the accurate determination of the P-wave arrival times from many different sensors for AE source location. The beamforming AE method described in this paper uses small (150 mm) aperture arrays, of 4–8 closely spaced sensors in order to make use of array signal processing techniques which have been developed for applications ranging from communications to imaging [12]. This methodology allows the direction of arrival of incoming AE waves to be determined and various wave phases which comprise an AE signal to be identified. Additionally, the array geometry reduces the need for high sampling rates and precise time synchronization between spatially distant sensors. This permits the use of wireless sensor networks for beamforming analyses, which will lower the cost and increase the flexibility of the monitoring system.

To motivate the use of beamforming as a tool for AE source location, the traditional time-difference-of-arrival (TDOA) method of estimating the location of AE sources is discussed in Section 2, and the difficulties associated with this method will be highlighted, especially with respect to AE source location on large concrete structures. In Section 3, array design considerations and assumptions made for the adaptation of beamforming methods to the problem of AE signal analysis in large concrete structures are discussed. Section 4 describes the theory behind beamforming and the analysis procedures relevant to beamforming AE. These include the variance scaled beam power formulation and VESPA (VElocity SPectral Analysis) process. The VESPA process is an illustrative signal discrimination technique used to identify the P-wave, R-wave, and their multiple reflections. The modeling assumptions made in the array design are then validated in Section 5 by means of simple experimental tests using artificial acoustic sources on a full-scale concrete structure. Finally, the results of this study are discussed to show the importance of this new tool for source location and signal discrimination in AE field applications and its potential for use in conjunction with wireless sensor networks.

2. Comparison between TDOA and beamforming analysis

The conventional AE source location method is commonly referred to as the time-difference-of-arrival (TDOA) scheme because it utilizes the differences in the times of arrivals of various wave modes in order to determine the source coordinates via triangulation [13]. In acoustic emission work, the arrivals of different wave modes are not easily identifiable and are often merged together with reflections. Consequently, only the arrival time of the fastest propagating P-wave, which is preceded by relative quiescence, can be accurately determined for use in AE source location schemes. For computation efficiency, the TDOA source location method is typically formulated as an inverse problem which relies on the very accurate determination of arrival times and usually employs iterative analysis routines to solve this nonlinear localization problem [14,15]. Due to its construction as an inverse problem, small errors in the estimated arrival times often equate to large distances in physical space (indicative of an ill-posed inverse problem) especially at ‘blind spots’ in the array geometry [16–18].

Most of the difficulties implicit in the TDOA location schemes are due to the inability to accurately detect the onset of the initial P-wave arrival and the unpredictable propagation and amplification of these errors in the inverse formulation of the problem. A significant amount of research has been performed in an attempt to improve the accuracy of automated P-wave arrival time picking algorithms [19–21], but for stress waves traveling through concrete this is an especially challenging problem. When propagating through concrete, an initially sharp stress wave pulse will become smoothed and broadened due to the frequency-dependent nature of scattering and intrinsic attenuation which is always present in concrete [22,23]. Fig. 1 illustrates the change of an AE signal as it travels through concrete, and Fig. 2 shows the power spectral estimates of these signals compared with the power spectrum of the present noise signal, all recorded by the same sensor (additional experimental details are described in Section 5). The three waveforms were generated by similar sources (the Hsu pencil lead break, described in Section 5) but have been recorded at different distances from the source (0.25, 1.5, and 3.8 m). Fig. 1(b) shows the first arrivals of the three waves at a greater time magnification. It is apparent from studying Fig. 1 that as the distance from the source to the receiver increases, the signal becomes more spread out in time, loses sharpness (higher frequencies), and the P-wave signal-to-noise ratio decreases to unity. Thus, at great distances, the first P-wave arrival becomes increasingly difficult to detect with accuracy and confidence.

These propagation effects render TDOA source location techniques ineffective for most AE signals which have propagated more than a meter through concrete. In these circumstances, an automatic picking algorithm (e.g. a threshold

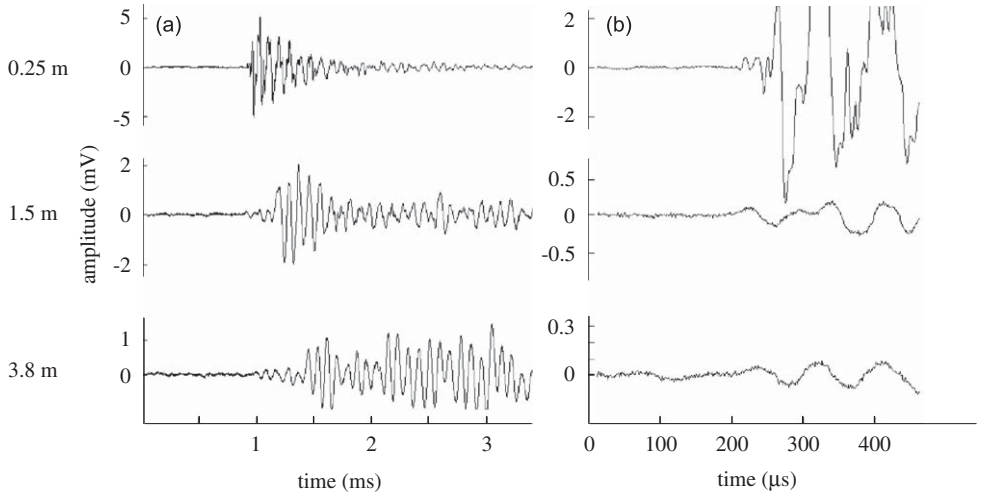

Fig. 1. Waveforms from similar AE sources located at varying distances from the same sensor, and (b) the same waveforms with greater time magnification.

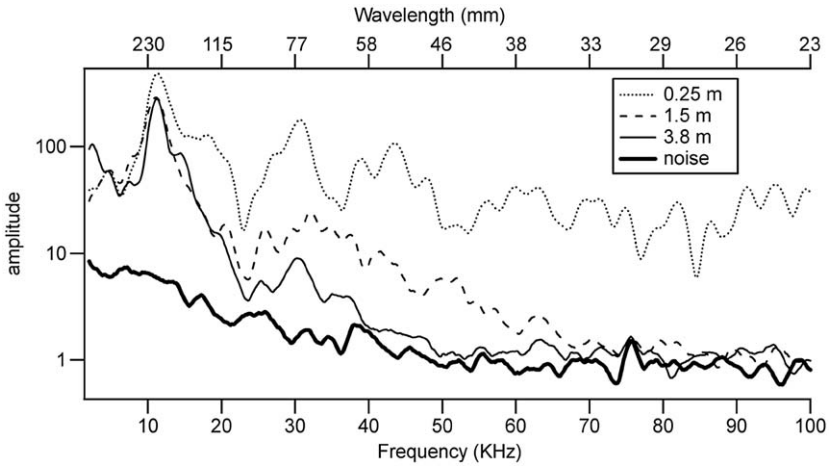

Fig. 2. Frequency spectra from the same three waveforms shown in Fig. 1 compared with the noise spectra. The wavelengths corresponding to each frequency are shown for reference (based on 2300 m/s Rayleigh wave velocity).

picker or Akaike Information Criterion (AIC) picker [21]) may incorrectly choose the arrival of surfaces waves, S-waves, or of reflections, which will cause the TDOA source location method to fail [24]. Due to the limited range at which arrival times of P-waves can be accurately detected, a structure must have a dense population of sensors in order to insure that the P-wave can be clearly detected by at least three sensors (the minimum number needed for source location in two dimensions using the TDOA method). In large concrete structures the required sensor array is extremely expensive and time consuming to install.

Instead of using a distributed array, the beamforming AE method relies on a small array of sensors spaced closely together so that, in the frequency range of interest (less than 50 kHz), all sensors will detect AE waves which have propagated along similar paths, and have been affected by similar attenuation and scattering. In the beamforming AE method, the direction of arrival of the AE waves can be determined simply from the relative time delays of similarly shaped signals recorded by neighboring sensors. This feature imposes the requirement that all sensors must have identical amplitude and phase response.

A number of different wave modes can propagate through a structure as a result of AE activity. These include P-waves, S-waves, and guided waves such as Rayleigh waves. As the plate thickness becomes small compared with the wavelengths of interest, the Rayleigh waves will degenerate into dispersive Lamb waves [25] which can also used for source location [26], but for the plate thicknesses and wavelengths relevant to AE analyses on thick civil engineering structures, the degenerate wave velocities will deviate from the Rayleigh wave speed by no more than about 20%. In the beamforming AE method, not only the P-wave, but all direct waves can be used for direction-of-arrival estimates. Rayleigh waves are confined to the surface of the specimen; therefore, geometrical spreading causes their amplitude to decay as $r^{-1/2}$ instead

of r^{-1} as is the case for P- and S-waves [27]. Consequently, at reasonable distances from the source, R-wave amplitudes will be significantly larger than the P-wave amplitudes. This feature allows the effective range of the beamforming array to be greater than for a TDOA source location scheme.

3. Array design and parameter sensitivity

This section describes assumptions and design requirements for AE beamforming arrays for locating AE sources on large and thick, plate-like, reinforced concrete structures (e.g. bridge decks and walls). Design considerations are predominantly governed by the characteristics of the expected AE sources and resulting wave fields such as the expected wavelengths and directions of arrival.

3.1. AE wavelengths in concrete

Concrete's effect on the frequency content (and consequently the wavelengths) of AE signals is illustrated in Fig. 2. From the figure it can be seen that as the stress waves propagate further and further through the concrete, the signals become effectively band limited to lower and lower frequencies (i.e. concrete is effectively a low pass filter) [22,23]. After traveling only 1.5 m through concrete, acoustic emissions which were initially rich in high frequencies have been attenuated such that 98% of the signal energy (above the noise level) is carried by frequencies under 25 kHz. For this work it was assumed that the array is intended to be used for locating AE sources at a range of one to four meters, therefore the majority of the energy contained in the AE will be carried at frequencies no greater than about 25 kHz, and the array must be designed to accommodate wavelengths down to about 85 mm.

3.2. Sensitivity to source parameters

For thick, plate-like structures it is most convenient to fix the sensors to one face of the structure, thus planar arrays will be considered. For a planar array, the direction of arrival cannot be uniquely determined. Instead, it depends on two parameters: the azimuthal angle of arrival and the horizontal slowness. Horizontal slowness, p, is defined as

$$p = \frac{\sin(\phi)}{c} \tag{1}$$

where c is the propagation velocity and ϕ the angle of incidence measured from the normal of the plane of the array (defined from 0° to 90°). If the propagation velocity is known the angle of incidence may be determined, and vice versa.

The sensitivity of a sensor array to a given source parameter can be studied by considering the trigonometric relationships which relate time delays between waves felt by neighboring sensors in the array to source characteristics [28] listed in a vector known as the steering vector **s**. Consider, for example, an n-element planar circular array of radius $a/2$ where each sensor is located at some azimuthal angle γ_i from the first sensor, shown (for n=4) in map view in Fig. 3(a) and side view in (b). If the array is initially steered to accept plane waves ($r=\infty$) arriving at propagation velocity c and an azimuth of 0 and incidence angle of 90° (steering vector **s**=(∞, c, 0°, 90°)) then the changes in time delays di(s) with respect to changes in azimuth and angle of incidence can be quantified:

$$\Delta d_i(\infty, c, 0-\Delta\theta, 90) = \frac{a}{2c}(\alpha - \cos(\Delta\theta) + \cos(\gamma_i + \Delta\theta)) \tag{2}$$

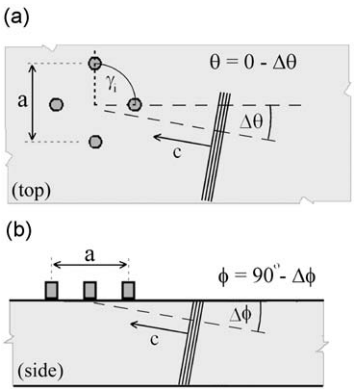

Fig. 3. (a) top view and (b) side view of a uniformly space circular planar array, of aperture a, on a plate-like structure with a plane wave arriving at an azimuth of 0–$\Delta\theta$° and an incidence angle of 90–$\Delta\phi$°.

$$\Delta d_i(\infty, c, 0, 90-\Delta\phi) = \frac{a}{2c}\alpha(1-\cos(\Delta\phi)) \tag{3}$$

where α=1−cos(γ_i), $\Delta\theta$ is the change in azimuthal angle, and $\Delta\phi$ is the change in incidence angle (deg).

In thick plate-like structures, the distances in the plane of the plate are large (several meters) compared with distances normal to the plate (less than 1 m) so most waves will arrive at an angle of incidence greater than 75°. These equations show that under these conditions the array is relatively insensitive to changes in incidence angle. For a uniformly spaced circular array a 5° change in azimuth produces the same magnitude of time delays as a 24° change in incidence angle. It may therefore be assumed that $\phi \approx 90°$, and the slowness $p \approx 1/c$.

Waves impinging upon an array can be very nearly approximated as plane waves as long as the true source of the waves is located outside of some near field zone. The effect of the plane wave assumption can be quantified by

$$\Delta d_i(\infty - r, c, 0, 90) = \frac{1}{c}\left(\sqrt{(r - a\cos(\gamma_i)/2)^2 + (a\sin(\gamma_i)/2)^2} - r + a\cos(\gamma_i)/2\right) \tag{4}$$

which describes the change in delay which results from changing the array focus from plane waves (r=∞) to spherical waves emanating from a source located a distance r from the center of the array. For the above example (aperture=120 mm) the near field zone is less than 0.34 m in radius. AE sources within the near field zone will violate the plane wave assumption and incur changes in time delays comparable to those incurred from a 5° change in azimuth ($\Delta\theta$=5°). These trigonometric relationships show that the small aperture arrays proposed in this paper (80–150 mm diameter circular arrays) are much more sensitive to changes in azimuth than changes in slowness or range. Therefore, the task of source location can be reduced to finding the most likely azimuth of arrival based on the assumption of plane waves propagating close to the R-wave velocity and at an angle of incidence of 90°.

4. Beamforming analysis procedures

4.1. Theory of time delay beamforming

Time delay beamforming is a method of filtering in both time and space, and the analysis techniques are relevant to the study of signals generated by propagating waves. It has been used extensively in radar [29], sonar [28], and exploratory seismology [30,31], and has been utilized as a tool for noninvasive testing techniques for pipelines and pressure vessels [32,33]. It has been infrequently used for active damage detection in civil engineering materials [34,35], but it has not yet been applied to the method of acoustic emission.

In beamforming applications the user must assume that the characteristics of waves incident on the array are relatively constant normal to their direction of propagation [36]. Under this fundamental assumption, a signal recorded by one sensor in an array is expected to be a time-delayed replica of a signal recorded by a neighboring sensor in that array. AE sources are usually considered point sources, so the 'delayed replica' assumption is only valid if the distance between the source and sensors is large compared with the distance between neighboring sensors. The relatively delayed signals can be combined (or stacked) to form an array output

$$g(t, \mathbf{s}) = \sum_{i=1}^{n} u_i(t - d_i(\mathbf{s})) \tag{5}$$

where u_i is the output from the ith of n sensors and $d_i(\mathbf{s})$ is the delay required to account for the slightly different arrival time of the propagating wave at sensor i. The amount of delay $d_i(\mathbf{s})$, depends on the geometry of the array and the steering vector $\mathbf{s}$, which includes the parameters of the expected source and the resulting wave field, such as the direction of arrival of the waves, the range of the source, and the velocity of propagation of the incoming wave modes. By adjusting the steering vector, and therefore changing the signal delays, the array output can be algorithmically 'steered' or 'focused' so that waves arriving from one direction and at one speed will sum constructively while waves arriving from other directions and speeds will destructively interfere. If the signals are correlated and the noise is uncorrelated, the beamforming array output can be used to increase the signal to noise ratio through stacking.

In passive sensing applications such as AE, the direction of arrival of propagating waves is often unknown. The source and the propagating waves which result can be defined by a number of parameters (those found in the steering vector), and these parameters may be estimated from the beam-power, derived from the moving average of the square of the beamforming array output over time, defined

$$P(t, \mathbf{s}) = \int_{t-T/2}^{t+T/2} g(\tau, \mathbf{s})^2 \, \mathrm{d}\tau \tag{6}$$

where $g(\tau,d_i)$ is defined in Eq. (5). The moving average time window T=450 μs was chosen because it is long enough to capture the direct P- and R-waves but is sufficiently short to eliminate much of the power from later-arriving reflections.

The azimuthal direction of arrival of the AE waves was estimated by finding the maximum of power-versus-azimuth curve, such as those shown in Fig. 4. This curve is the maximum over time of Eq. (6), assuming r=∞, v=2300 m/s, ϕ=90, and

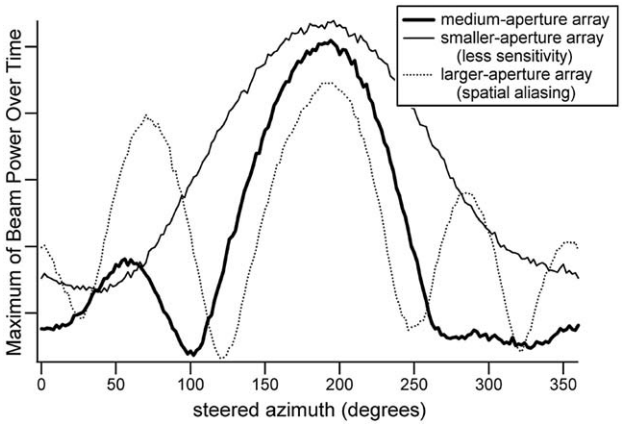

Fig. 4. Beam-power-versus-azimuth curves for arrays of varying aperture showing array sensitivity and spatial aliasing.

calculated for steered azimuths equally spaced over the entire range from 0° to 360°. The maximum of this curve (which ideally corresponds to the azimuthal direction of arrival of the direct waves), is taken to be the best estimate of the direction of the source. Noise that is always present in real AE signals introduces some roughness and uncertainty in the beam-power-versus-azimuth curves; therefore these curves are always smoothed before the maximum is estimated.

Three examples of power-versus-azimuth curves are shown in Fig. 4 for arrays of different apertures. The power-versus-azimuth curve from the medium-aperture array in Fig. 4 shows a main peak (or main lobe) located near 180°, corresponding to the true direction of arrival of the AE waves, and a smaller peak near 60° due to a smaller-amplitude reflection which arrives from a different azimuth. This figure shows that the variance of estimates of direction of arrival is inversely proportional to the size of the array [28]. In other words, if the aperture of the array is small (compared with the wavelengths of the AE), the array is less sensitive to changes in steered azimuth (the main lobe is broad). On the other hand, spatial aliasing, analogous to aliasing in the time domain, can occur when the array element spacing is too large for the characteristics of the short-wavelength signals to be accurately captured [37]. If the aperture of the array is increased (and the number of elements in the array is kept constant), the sensitivity of the array is increased at the cost of spatial aliasing. In this case the main lobe becomes narrower but side lobes become larger and can bias direction-of-arrival estimates. Therefore, it is desirable to design the largest array possible using as few elements as possible (to keep costs low) while still avoiding spatial aliasing.

In order to develop a robust AE source location technique based on beamforming, the array must be designed and the beam-power defined in such a way that beam-power is maximized when the array is steered in the correct direction and minimized when array is steered in an incorrect direction. Based on the requirement that the array must be designed to accommodate wavelengths down to about 85 mm, a 4–8 element circular planar array design with an aperture size of about 80–150 mm was chosen.

4.2. Beam power formulation

Many different formulations for beam-power are in common use. For example, the generalized cross-correlator function

$$P(t,\mathbf{s}) = \int_{t-T/2}^{t+T/2} \prod_{i=1}^{n} u_i(\tau - d_i(\mathbf{s}))\,\mathrm{d}\tau \tag{7}$$

can be used to estimate the direction of arrival as an alternate to Eq. (6). This estimator can optimally process data even when the noise spectra for each signal are different [38]. Another alternative is to replace Eq. (5) with an adaptive beamformer such as a minimum variance beamformer (Capon's beamformer) or a subspace-based method such as the MUSIC algorithm output [39]. These beamformers can be designed to have optimal performance when the spectra of both the signal and noise are known.

For simplicity, the data-independent beamforming power estimate (Eq. (6)) and variations described below were chosen because they perform well under broadband background noise [31] and are maximum likelihood estimators for the time delay if signal and white noise are uncorrelated [28].

For AE signals, multiple reflections often reach the sensor array at times later than the direct P- and R-wave arrivals. These reflections often arrive from a different azimuth than the direct arrivals and can bias the direction of arrival estimates. Performance improvement is gained by normalizing the beamforming array output (Eq. (5)) by the variance of

the individual beam components:

$$P_{\text{norm}}(t,\mathbf{s}) = \int_{t-T/2}^{t+T/2} \frac{g(\tau,\mathbf{s})^2}{\text{var}(\tau,\mathbf{s})}\,\text{d}t \tag{8}$$

where

$$\text{var}(\tau,\mathbf{s}) = \frac{1}{n-1}\sum_{i=1}^{n}(u_i(\tau - d_i(\mathbf{s})) - \overline{u}(\tau,\mathbf{s}))^2 \tag{9}$$

$$\overline{u}(\tau,\mathbf{s}) = \frac{1}{n}\sum_{i}^{n} u_i(\tau - d_i(\mathbf{s})) \tag{10}$$

This estimator penalizes beams whose components are not well correlated. This effectively increases the power of the direct waves compared with that of later-arriving reflections because direct arrivals typically reach the array before any reflections have muddied the wave field. This beam power formulation is particularly useful for the VESPA process.

4.3. VESPA process

In addition to its use as a method of AE source location, beamforming array processing can be used to discriminate between different types of signals based on the wave phases they contain. Acoustic emission signals contain multiple wave phases (P, S, R, etc.) which propagate at different velocities and arrive at the array at different times and decay differently with distance. Yet these different wave phases share similar frequency bands. The VESPA process is an illustrative method of spotlighting different wave phases in slowness and time [31,40,41]. The vespagrams shown in this paper serve as a means of illustrating the AE wave field, but are not well suited for parameter estimation.

The vespagram is constructed using the beam-power described in Eq. (8) and a moving average time window of 115 μs to provide enough temporal resolution such that the P- and R-waves remain distinct even for source ranges as small as 1 m. The steering vector **s** is systematically adjusted (altering the delays $d_i(\mathbf{s})$) so that the array is focused at a number of pre-assigned wave velocities while held at a fixed azimuth. In order to fully encompass all the wave modes expected to propagate in concrete, a set of wave velocities was selected at uniform increments in slowness over the range from 1500 to 6000 m/s. The fixed azimuth corresponds to the direction of the AE source which was previously estimated by the methods described above. Contours of constant beam-power are then drawn from the resulting three dimensional plot of beam-power versus slowness versus time.

A vespagram from a typical AE signal will contain a peak corresponding to the direct-P wave arrival at the P-wave velocity followed by a much larger peak corresponding to the direct R-wave arrival at a lower velocity. If the P- and R-wave velocities c_P and c_R are known, then a rough estimate of the range of the AE event

$$r = \frac{(t_R - t_P)c_R c_P}{c_P - c_R} \tag{11}$$

may be attained by extracting the P–R arrival time difference (t_R–t_P).

5. Experimental validation

In order to validate assumptions made for array design, a set of tests was conducted on a steel reinforced concrete bridge ramp at the University of Stuttgart, Germany, as shown in Fig. 5. The section of the bridge ramp tested has a thickness of 0.3 m and is 4 m wide (west–east) and 5 m long (north–south). The structure also has some visible spalling from the

Fig. 5. The reinforced concrete bridge ramp tested at the University of Stuttgart, Germany.

corrosion of steel reinforcing. An eight-element 120 mm diameter circular array was chosen for this test, and the array was placed 1.5 and 2 m from the east and north sides, respectively. Panametrics sensors V103 with broad sensitivity between 5 and 100 kHz were used to satisfy the requirement that all sensors in the array have identical amplitude and phase responses. The sensors were mounted to the underside of the concrete bridge with hot glue; no additional surface preparation or couplant was used. Signals were recorded using the TransOcto-Multichannel-AE system of the University of Stuttgart [42] at a sampling rate of 1 MHz for a total of 5000 data points, corresponding to record length 5 ms.

Artificial acoustic emissions, from the so-called Hsu source [43], were created by breaking a mechanical pencil lead on the surface of the concrete on the same plane as the sensor array. This artificial source is commonly used as a qualitative calibration procedure to verify sensor coupling, AE attenuation in the specimen, and source location capabilities [44,45]. The frequency content of this source is known [46] and it is assumed to be representative of typical AE in concrete. The performance of the array was evaluated for sources at a variety of ranges and azimuths by creating artificial acoustic emissions at 43 separate locations (ranging from 0.25 to 4 m from the sensor array). For each artificial acoustic emission signal recorded, the direction of arrival was estimated using the method described in Section 4 (from the maximum of the power-versus-azimuth curve, with $r=\infty$, v=2300 m/s, ϕ=90°). This estimate was then compared with the true direction of arrival calculated assuming a direct ray path from the location of the artificial source to center of the sensor array.

Fig. 6 shows the difference (deg) between azimuthal direction of arrival estimates and the true direction of arrival as a function of range for artificial acoustic emissions input at locations of varying azimuth and range. By using a subset of the original signals the beamforming source location scheme was tested for both an eight and a four element circular array of the same aperture. The squares represent individual errors for the 43 artificial acoustic emission locations using the full eight-element 60 mm radius circular array, and the dashed lines indicate the 95% confidence intervals for these errors. The triangles and dotted lines represent the individual errors and 95% confidence intervals using the signals from only four of the eight sensors. When all eight elements are used, the direction of arrival was estimated with 95% confidence to be plus or minus 10° using the normalized beam-power. Using half as many sensors, the 95% confidence bounds were within 14°.

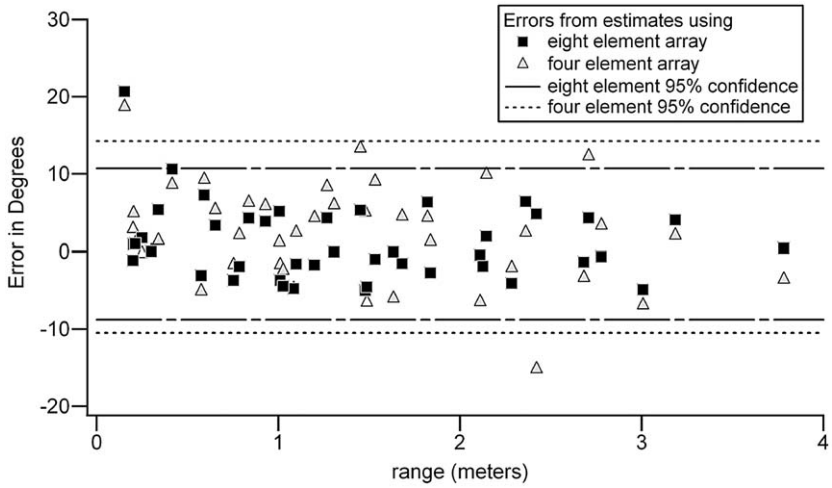

Fig. 6. The accuracy of azimuthal direction of arrival estimates as a function of range.

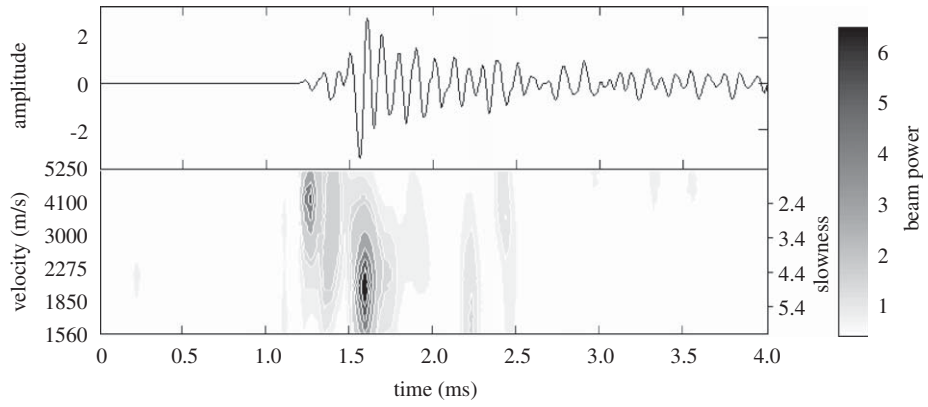

Fig. 7. Array output and vespagram for an AE event located 1.5 m from the sensor array.

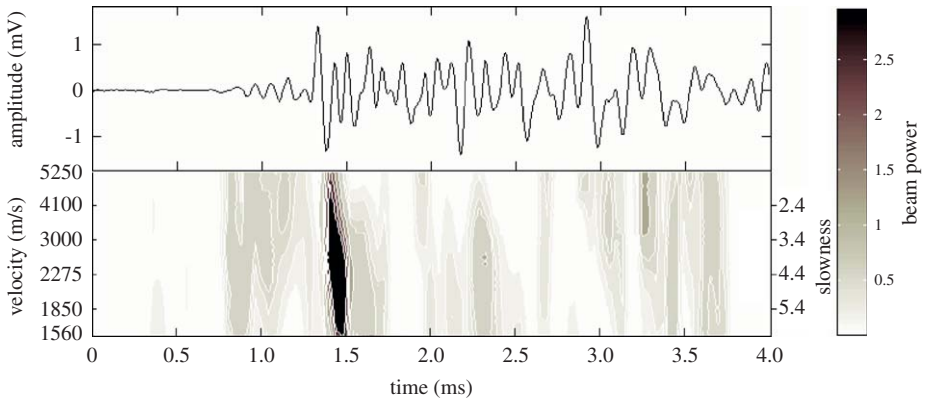

Fig. 8. Array output and vespagram for an AE event located 3.8 m from the sensor array.

In addition to using the beamforming array for source location, further signal discrimination was attained using the VESPA process. Fig. 7 presents the VESPA process for one artificial acoustic emission (pencil lead break) compared with the beamforming array output (Eq. (5)). As shown in the figure, the P-wave arrives first at a velocity of about 4000 m/s while a stronger R-wave arrives at a later time and at a velocity of approximately 1900–2300 m/s. The VESPA process highlights the insensitivity of the sensor array to changes in steered slowness (i.e. the array and vespagram cannot be used for accurate velocity or incidence angle estimation).

The vespagram shown in Fig. 7 is from an AE source located 1.5 m away from the sensor array. At this distance the P- and R-waves have separated by about 300 μs. The vespagram shown in Fig. 8 is from an AE source located 3.8 m away from the array, for which the P- and R-waves have separated by approximately 700 μs. The ratio of P-wave to R-wave amplitude for this AE event is much smaller than the P- to R-wave amplitude ratio shown in Fig. 7, because the P-wave decays more rapidly with distance than the R-wave.

6. Discussion

Both the TDOA and beamforming localization schemes rely on certain modeling assumptions. As described in Section 2, for AE sources located more than a meter away from a sensor the assumption of accurate P-wave arrival time determination is grossly violated. The beamforming source location method operates under a different set of assumptions (e.g. the 'delayed replica' assumption) which are much more appropriate for AE applications in large concrete structures where ray paths from source to receiver are large, the P-wave amplitude is small, and angles of incidence are close to 90°.

The test results on the concrete bridge ramp show that the modeling assumptions made in the array design can be considered valid for the test case, and that the azimuthal direction of artificial AE sources can be accurately determined (to within 14°) for sources located up to 4 m from the 4 sensor array. This level of precision is sufficient for most field applications. Beamforming localization can be seen as a tool which points the user toward one particular direction from which increased AE activity takes place, either in the location of a previously known flaw or a new zone of damage. A rough range estimate found from Eq. (11) could provide a means of further localization for well-defined AE sources such as the one shown in Fig. 7. The range of effectiveness and the reliability of the beamforming AE techniques can be greatly improved by coupling two or more beamforming sensor arrays. For example, if the direction of the source can be determined by two or more arrays, the source location can be identified in two dimensions [7,47].

The tests on the concrete bridge ramp indicate that the azimuth of the AE source could be roughly determined even at ranges where it is impossible to accurately detect a P-wave. For example, the AE depicted in Fig. 8 traveled nearly 4 m to the sensor array, yet the bearing of the source was located to within a few degrees of the true direction. One sensor's recorded signal from this same AE is shown in Fig. 1 (the lower signal), and it is probably impossible to identify the P-wave with an automatic picking algorithm with an error of less than 300 μs. Picking errors of that magnitude render an accurate TDOA source location estimate impossible.

There are some constraints to which the beamforming array must adhere. For example, because the beamforming method relies on the comparison of the shape of signals it is absolutely crucial that all sensors in the array have identical amplitude and phase responses, which is not necessarily needed for TDOA source location schemes. Additionally, the beamforming array must be of a relatively small aperture to ensure that spatial aliasing is avoided and that ray paths from source to sensor are similar enough that the stress waves experience the same propagation effects (i.e. scattering, attenuation, etc.). Arguments presented in Section 3 have shown that the angle of incidence of the arriving waves cannot be accurately estimated with arrays of this size, and it is unreasonable to assume that azimuth can be estimated to a precision better than $\pm 5^\circ$ due to the broadness of the main lobe in the beam-power-versus-azimuth curve shown in Fig. 4 and noise

which is always present in AE signals. In theory, the beamforming localization method cannot be as precise as the TDOA method. In practice, however, this limitation is dwarfed by practical limitations of the TDOA method.

With the proper anti-alias filtering, the band-limited nature of the AE signals which have propagated through concrete facilitates the use of lower sampling rates (50 kHz, say). By combining a lower sampling rate with the use of digital interpolation beamforming algorithms (e.g. Pridham and Mucci [48]), the costs of data acquisition systems can be reduced without loss of utility.

The new-found popularity of low-power wireless sensor networks has led to products that are considerably less expensive and easier to install than wired systems, and can be easily adapted and scaled to different types of structures [49,5]. To date, stringent requirements such as high sampling rates and precise time synchronization between sensor nodes have prevented AE analysis from being integrated into wireless sensor networks. A constraint of the TDOA scheme is the requirement that all recorded signals be synchronized to a common time, with accuracy on the order of a few microseconds. This level of accuracy in a multihop wireless sensor network greatly increases the overall power requirements [50], and at present the needed synchronicity is not readily available [48]. By connecting a small aperture array of four sensors to one wireless mote with a very accurate common clock, the task of synchronizing spatially distant sensors is avoided. Coupled beamforming arrays are required to be time synchronized only to the rate at which individual events in a series of successive AE can be identified amid the noise of the previous AE events. For the frequency range found in AE in large concrete structures, quiescence is reached after about 5–20 ms, therefore there is no need for a time synchronicity between separate beamforming arrays of better than a few milliseconds. Beamforming AE analyses can be performed on board the wireless mote in order to reduce the amount of data transmission required from kilo samples to 2 or 3 bytes. Trading transmission for computation can reduce the overall power requirements by at least an order of magnitude [49]. Wireless AE coupled with beamforming techniques may be the future of condition monitoring in large civil engineering structures.

7. Conclusions

While acoustic emission analysis has been effectively used as a research tool in laboratory settings and as a qualitative monitoring tool for in-situ non-destructive evaluation, a robust and quantitative application of the method for use on civil infrastructure has not yet been achieved. In order for AE analysis to be successful in field applications different approaches must be used in order to gain meaningful and quantitative information from uncertain and noisy data. It is too costly to implement a large, distributed array of sensors capable of high resolution source location via the TDOA method. The goal of AE beamforming is to provide a reliable but less precise method of damage localization for AE applications on large concrete structures, so that more detailed non-destructive testing procedures can be applied at the proper location.

A small aperture array (80–150 mm for many applications) must be used in this method for spatial aliasing to be avoided. Using trigonometric relationships, it was found that for angles of incidence close to 90° the small aperture array is relatively insensitive to changes in incidence angle and range (compared with changes in azimuth), which simplifies source location in three dimensions to an estimation of angle of arrival. Following a conventional delay-and-sum beamforming formulation, a beamforming localization scheme was effectively applied to artificial acoustic emission signals collected on a full-scale reinforced concrete structure, and the direction of arrival of these sources was calculated to within 14° of the true direction at ranges of up to 4 m with an array of only four sensors. The VESPA process was constructed using a variance-scaled beam power formulation specifically designed for AE signals. This analysis tool was used to describe wave phase arrival time and amplitude information which can provide a means of additional signal discrimination.

While the TDOA method is generally more precise than the beamforming localization scheme, at distances greater than 1 m the advantages of the TDOA method become moot since it relies on P-wave arrival times which are impossible to accurately determine. The beamforming source location technique presented in this paper circumvents many of the traditional problems presented by the TDOA source location procedure. Because precise P-wave arrival time information is no longer required, sampling rates can be reduced by utilizing the band-limited nature of the AE signals in concrete. By arranging the sensors into small clusters the need for precise time synchronization between spatially distance sensors is also eliminated. These characteristics make beamforming AE well suited for use with wireless sensor networks.

Acknowledgements

The authors gratefully acknowledge the help of Gerhard Bahr, Panagiotis Chatzichrisafis, and Anne Jüngert with the experimental work at the University of Stuttgart, Germany. This work was funded by NSF-GRF and NSF Grant CMS-0624985.

References

[1] A. Pollock, B. Smith, Stress-wave-emission monitoring of a military bridge, *Nondestructive Testing* 5 (6) (1972) 348–353.
[2] C. Scruby, H. Wadley, Assessment of acoustic emission for nuclear pressure vessel monitoring, *Progress in Nuclear Energy* 11 (3) (1983) 275–297.
[3] M. Sison, J. Duke, G. Clemena, M. Lozev, Acoustic emission: a tool for the bridge engineer, *Materials Evaluation* 54 (8) (1996) 888–900.

[4] T. Fowler, T.L. Yépez, C. Barnes, Acoustic emission monitoring of reinforced and prestressed concrete structures, in: R. Medlock, D. Laffrey (Eds.), *Proceedings of the SPIE—Structural Materials Technology III: An NDT Conference*, Vol. 3400, San Antonio, 1998, pp. 281–298.
[5] C. Grosse, S. Glaser, M. Krüger, Condition monitoring of concrete structures using wireless sensor networks and MEMS, in: M. Tomizuka, C. Yun, V. Giurgiutiu (Eds.), *Proceedings of the SPIE, Sensors and Smart Structures and Materials 2006: Sensors and Smart Structures Technologies for Civil, Mechanical and Aerospace Systems*, San Diego, Vol. 6174, 2006, 61741C pp.
[6] K. Kim, W. Sachse, Characteristics of an acoustic emission source from a thermal crack in glass, *International Journal of Fracture* 31 (1986) 211–231.
[7] B. Ferguson, L. Criswick, K. Lo, Locating far-field impulsive sound sources in air by triangulation, *Journal of the Acoustical Society of America* 111 (1) (2002) 104–116.
[8] C. Scruby, K. Stacey, K.G. Baldwin, Defect characterization in three dimensions by acoustic emission, *Journal of Physics D* 19 (1986) 1597–1612.
[9] M. Ohtsu, K. Ono, AE source location and orientation determination of tensile cracks from surface observation, *NDT International* 21 (1988) 143–150.
[10] S. Glaser, P. Nelson, Acoustic emissions produced by discrete fracture in rock, *International Journal of Rock Mechanics and Mining Sciences and Geomechanics Abstracts* 29 (1992) 253–265.
[11] C. Grosse, H. Reinhardt, T. Dahm, Localization and classification of fracture types in concrete with quantitative acoustic emission measurement techniques, *NDT&E International* 30 (1996) 223–230.
[12] B. Van Veen, K. Buckley, Beamforming: a versatile approach to spatial filtering, *IEEE ASSP Magazine* 5 (2) (1988) 4–24.
[13] J. Baron, S. Ying, Acoustic emission source location, in: R. Miller, P. McIntire (Eds.), *Nondestructive Testing Handbook Second Edition, Vol. 5: Acoustic Emission Testing, American Society for Nondestructive Testing*, 1987, pp. 136–154.
[14] M. Salamon, G. Wiebols, Digital location of seismic events by an underground network of seismometers using the arrival times of compressional waves, *Rock Mechanics* 6 (1974) 141–166.
[15] S. Stein, M. Wysession, *An Introduction to Seismology, Earthquakes, and Earth Structure*, Blackwell, Massachusetts, 2003.
[16] S. Spencer, The two-dimensional source location problem for time differences of arrival at minimal element monitoring arrays, *Journal of the Acoustical Society of America* 121 (6) (2007) 3579–3594.
[17] M. Ge, H. Hardy, The role of transducer array geometry in AE/MS source location, *Fifth Conference on Acoustic Emission/Microseismic Activity in Geologic Structures and Materials*, Pennsylvania State University, June 11–13, 1991, pp. 561–571.
[18] B. Schechinger, Schallemissionsanalyse als Überwachungsinstrument für Schädigung in Stahlbeton (Acoustic Emission Analysis as a Monitoring Tool for Reinforced Concrete Deteriorations), PhD Thesis, Eidgenössische Technische Hochschule Zürich (ETH), Zürich, Switzerland, 2005.
[19] M. Baer, U. Kradolfer, The two-dimensional automatic phase picker for local and teleseismic events, *Bulletin of the Seismological Society of America* 77 (4) (1987) 1437–1445.
[20] E. Landis, C. Ouyang, S. Shah, Automated determination of first P-wave arrival and acoustic emission source location, *Journal of Acoustic Emission* 10 (1992) S97–S103.
[21] J. Kurz, C. Grosse, H. Reinhardt, Strategies for reliable automatic onset time picking of acoustic emissions and of ultrasound signals in concrete, *Ultrasonics* 43 (2005) 538–546.
[22] Y. Kim, S. Lee, H. Kim, Attenuation and dispersion of elastic waves in multi-phase materials, *Journal of Physics D* 24 (10) (1991) 1722–1728.
[23] E. Landis, S. Shah, Frequency-dependent stress wave attenuation in cement-based materials, *Journal of Engineering Mechanics* 121 (1995) 737–743.
[24] M. Ge, P. Kaiser, Interpretation of physical status of arrival picks for microseismic source location, *Bulletin of the Seismological Society of America* 80 (1990) 1643–1660.
[25] J. Krautkramer, H. Krautkramer, *Ultrasonic Testing of Materials*, Springer, Berlin, 1990.
[26] M. Gorman, W. Prosser, AE source orientation by plate wave analysis, *Journal of Acoustic Emission* 9 (4) (1991) 283–288.
[27] K. Aki, P. Richards, *Quantitative Seismology—Theory and Methods*, Freeman, San Francisco, 1980.
[28] C. Carter, Time delay estimation for passive sonar signal processing, *IEEE Transactions on Acoustic Speech and Signal Processing* ASSP-29 (3) (1981) 463–470.
[29] S. Haykin, Radar processing for angle of arrival estimation, in: S. Haykin (Ed.), *Array Signal Processing*, Prentice-Hall, New Jersey, 1985, pp. 194–292.
[30] J. Justice, Array processing in exploratory seismology, in: S. Haykin (Ed.), *Array Signal Processing*, Prentice-Hall, New Jersey, 1985, pp. 6–14.
[31] E. Kelly, Response of seismic arrays to wideband signals, Lincoln Laboratory Technical Note, 1967-30, 1967.
[32] W. Luo, J. Rose, Phased array focusing and guided waves in a viscoelastic coated hollow cylinder, *Journal of the Acoustical Society of America* 121 (4) (2007) 1945–1955.
[33] G. Santoni, L. Yu, B. Xu, V. Giurgiutiu, Lamb wave-mode tuning of piezoelectric wafer active sensors for structural health monitoring, *Journal of Vibration and Acoustics—Transactions of the ASME* 129 (6) (2007) 752–762.
[34] S. Sundararaman, D. Adams, E. Rigas, Structural damage identification in homogeneous and heterogeneous structures using beamforming, *Structural Health Monitoring* 4 (2) (2005) 171–190.
[35] L. Azar, S. Wooh, Experimental characterization of ultrasonic phased arrays for nondestructive evaluation of concrete structures, *Materials Evaluation* (1999) 135–140.
[36] D. Dudgeon, Fundamentals of digital array processing, *Proceedings of the IEEE* 65 (6) (1977) 898–904.
[37] D. Johnson, D. Dudgeon, *Array Signal Processing: Concepts and Techniques PTR*, Prentice-Hall, New Jersey, 1993.
[38] W. Hahn, Optimum signal processing for passive sonar range and bearing estimation, *Journal of the Acoustical Society of America* 58 (1) (1975) 201–207.
[39] H. Krim, M. Viberg, Two decades of array signal processing research, *IEEE Signal Processing Magazine* 13 (4) (1996) 67–94.
[40] D. Doornbos, E. Husebye, Array analysis of PKP phases and their precursors, *Physics of the Earth and Planetary Interiors* 5 (1972) 387–399.
[41] S. Rost, C. Thomas, Array seismology: methods and applications, *Review of Geophysics* 40 (3) (2002) 1–27.
[42] J. Kurz, G. Bahr, C. Grosse, Entwicklung eines Transientenrekorders für die Schallemissionsanalyse. (Development of a transient recorder for acoustic emission analysis), in: R. Jamal, H. Jaschinski (Eds.), *Virtuelle Instrumente in der Praxis (Virtual Instruments in Practice)*, Hüthig, Munich, 2005, pp. 140–144.
[43] N. Hsu, Acoustic Emission Simulator, U.S. Patent No. 4018084, 1977.
[44] M.A. Hamstad, Acoustic emission signals generated by monopole (pencil lead break) versus dipole sources: finite element modeling and experiments, *Journal of Acoustic Emission* 25 (2007) 92–106.
[45] D. Eitzen, F. Breckenridge, R. Clough, E. Fuller, N. Hsu, J. Simmons, Fundamental developments for quantitative acoustic emission measurements, Interim Report NP-2089, prepared for Electric Power Research Institute, 1981.
[46] F. Breckenridge, T. Proctor, N. Hsu, S. Fick, D. Eitzen, Transient sources for acoustic emission work, in: K. Yamaguchi, H. Takahashi, H. Niitsuma (Eds.), *Progress in Acoustic Emission V*, The Japanese Society for NDI, Sendai, Japan, 1990, pp. 20–37.
[47] S. Holland, D. Chimenti, R. Roberts, M. Strei, Locating air leaks in manned spacecraft using structure-borne noise, *Journal of the Acoustical Society of America* 121 (6) (2006) 3484–3492.
[48] R. Pridham, R. Mucci, Digital interpolation beamforming for low-pass and bandpass signals, *Proceedings of the IEEE* 67 (6) (1979) 904–919.
[49] J. Lynch, K. Loh, A summary review of wireless sensors and sensor networks for structural health monitoring, *Shock and Vibration Digest* 38 (2) (2006) 91–128.
[50] K. Pister, Personal communication, 2008.